Research paper

A higher-order perturbation analysis of the nonlinear Schrödinger equation

J. Bonetti [a,c], S.M. Hernandez [a], P.I. Fierens [b,c,*], D.F. Grosz [a,c]

[a] *Grupo de Comunicaciones Ópticas, Instituto Balseiro, Argentina*
[b] *Instituto Tecnológico de Buenos Aires, Argentina*
[c] *Consejo Nacional de Investigaciones Científicas y Técnicas (CONICET), Argentina*

Keywords:
Optical fibers
Noise
Modulation instability

A B S T R A C T

A well-known and thoroughly studied phenomenon in nonlinear wave propagation is that of modulation instability (MI). MI is usually approached as a perturbation to a pump, and its analysis is based on preserving only terms which are linear on the perturbation, discarding those of higher order. In this sense, the linear MI analysis is relevant to the understanding of the onset of many other nonlinear phenomena, such as supercontinuum generation, but it has limitations as it can only be applied to the propagation of the perturbation over short distances.

In this work, we propose approximations to the propagation of a perturbation, consisting of additive white noise, that go beyond the linear modulation instability analysis, and show them to be in excellent agreement with numerical simulations and experimental measurements.

1. Introduction

Pulse propagation in single-mode lossless nonlinear fibers is modeled by the Nonlinear Schrödinger Equation (NLSE) [1]

$$\frac{\partial A}{\partial z} - i\hat{\beta}A = i\hat{\gamma}A|A|^2. \tag{1}$$

$A(z, T)$ is the pulse envelope, z is the direction of propagation and T is the time referred to a co-moving frame with group velocity $v_g = \beta_1^{-1}$ (i.e., $T = t - z\beta_1$). Linear dispersion is modeled by the operator $\hat{\beta}$, while $\hat{\gamma}$ is related to the third-order susceptibility:

$$\hat{\beta} = \sum_{k\geq 2} \frac{i^k \beta_k}{k!}\frac{\partial^k}{\partial T^k}, \quad \hat{\gamma} = \sum_{k\geq 0} \frac{i^k \gamma_k}{k!}\frac{\partial^k}{\partial T^k}. \tag{2}$$

We must note that, for the sake of simplicity, we have omitted the contribution of the stimulated Raman response of the medium. Furthermore, we have not included any noise source such as spontaneous Raman emission.

Analytical solutions of Eq. (1) are known in a variety of simplified cases. For instance, solitonic solutions can be found by means of the inverse-scattering method originally proposed by Zakharov and Shabat [2] (see also, e.g., [3]), but only

* Corresponding author at: Mathematics and Physics, Av. Eduardo Madero 399, Ciudad Autónoma de Buenos Aires C1106ACD, Argentina.
E-mail address: pfierens@itba.edu.ar (P.I. Fierens).

under some simplifications such as no higher-order dispersion ($\beta_k = 0$ for $k \geq 3$). An important family of periodic solutions, known as Akhmediev breathers [4], has attracted attention in relation to supercontinuum generation and rogue waves [5,6]. Although Akhmediev breathers were originally found for low-dispersion cases, Eq. (1) has been found to be integrable in more complex cases (see, for example, [7–11] and references therein). However, the number of exactly integrable variations of the NLSE is still very limited.

Although exact solutions of simplified versions of Eq. (1) provide important insight into many features of the propagation of pulses in nonlinear fibers, they do not provide a precise description in general. For this reason, the NLSE is usually studied by means of simulations based on efficient algorithms such as split-step Fourier (SSF) [1] or a fourth-order Runge-Kutta in the interaction picture (RK4IP) [12].

In this work, we put forth a perturbation analysis of the Eq. (1) when a continuous-wave (CW) laser pumps the nonlinear fiber. The CW pump is always accompanied by technical and quantum noise and we focus on the noise propagation along the fiber. Our goal is not to propose an efficient methodology that can substitute numerical simulations of the nonlinear Schrödinger equation, but to introduce approximate expressions that can provide a more intuitive and comprehensive understanding of the main processes involved in higher-order modulation instability.

One possibility is to study noise propagation as a perturbation to the CW. The first-order perturbation or linear stability analysis is related to the study of the modulation instability (MI) phenomenon [4,5,13–23,23–29] (see also Chapter 5 of Ref. [1] and references therein.) Exact solutions of MI accounting for a full model of the NLSE, including the Raman response and the dependence of the nonlinear parameter with frequency, have been developed [30,31]. The particular case of the propagation of additive noise has been dealt with in the literature (see, e.g., [32,33]). Note, however, that the wave propagation analysis of a noisy CW pump in a MI setting has several limitations. The continuous-wave pump is assumed undepleted and, hence, the results are only valid over short propagation distances. Furthermore, as it is a first-order perturbation analysis, it disregards the 'cascading effect' of four-wave mixing, in the sense that perturbations to the pump can as well act as pumps themselves once they have attained enough power. One alternative to incorporate such cascading effect is to solve the NLSE through Picard's iterations. Resulting expressions are, nevertheless, not easily tractable and even their numerical evaluation may turn out to be an expensive computational effort as compared to pure numerical solutions obtained from the usual SSF or RK4IP algorithms. For this reason, we put forth several simplifications that allow an analysis of higher-order perturbations. The validity of these simplifications is tested through numerical simulation and experimental measurements.

We must note that there are alternative approaches which are related to ideas presented in this work. In particular, many tools have been developed for the statistical analysis of optical wave turbulence (see, e.g., [34–38]).

The remaining of this paper is organized as follows. In Section 2 we develop a higher-order perturbation analysis of the nonlinear Schrödinger equation and motivate the simplifications that allow tractability. We validate our approach with experimental results and numerical simulations in Section 3. Finally, we present some conclusions and lines of future work in Section 4.

2. Perturbation analysis

Let us again consider the nonlinear Schrödinger equation. It is useful to normalize the propagation distance as $\zeta = \gamma_0 P_0 z$. We study the propagation of a small perturbation $a(\zeta, T)$ to the stationary solution of Eq. (1), i.e., we consider $A(\zeta, T) = \sqrt{P_0}[1 + a(\zeta, T)]e^{i\zeta}$. Fourier transformation (with respect to time T) leads to the following coupled differential equations

$$i\partial_\zeta \tilde{a}(\zeta, \Omega) + B(\Omega)\tilde{a}(\zeta, \Omega) + \tilde{\gamma}(\Omega)\overline{\tilde{a}(\zeta, -\Omega)} = -\gamma(\Omega)\tilde{N}(\tilde{a}(\zeta, \Omega)), \tag{3}$$

$$-i\partial_\zeta \overline{\tilde{a}(\zeta, -\Omega)} + B(-\Omega)\overline{\tilde{a}(\zeta, -\Omega)} + \tilde{\gamma}(-\Omega)\tilde{a}(\zeta, \Omega) = -\gamma(-\Omega)\overline{\tilde{N}(\tilde{a}(\zeta, -\Omega))}, \tag{4}$$

where $\tilde{a}(\zeta, \Omega)$ is the Fourier transform of $a(\zeta, T)$, $B(\Omega) = \tilde{\beta}(\Omega) + 2\tilde{\gamma}(\Omega) - 1$,

$$\tilde{\beta}(\Omega) = \frac{1}{\gamma_0 P_0} \sum_{m=2}^{M} \frac{(-1)^m}{m!} \beta_m \Omega^m, \qquad \tilde{\gamma}(\Omega) = \frac{1}{\gamma_0} \sum_{n=0}^{N} \frac{(-1)^n}{n!} \gamma_n \Omega^n, \tag{5}$$

$$\tilde{N}(\tilde{a}) = \tilde{a}(\zeta, \Omega) * \overline{\tilde{a}}(\zeta, -\Omega) + \tilde{a}(\zeta, \Omega) * \left[\tilde{a}(\zeta, \Omega) + \overline{\tilde{a}}(\zeta, -\Omega)\right] + \tilde{a}(\zeta, \Omega) * \tilde{a}(\zeta, \Omega) * \overline{\tilde{a}}(\zeta, -\Omega). \tag{6}$$

2.1. Linear stability analysis

Analysis of modulation instability (MI) proceeds by neglecting the nonlinear terms in Eqs. (3)–(4). Let us assume that $\tilde{a}(0, \Omega)$ is a noisy perturbation such that

$$\left\langle \tilde{a}(0, \Omega) \right\rangle = 0, \qquad \left\langle \tilde{a}(0, \mu)\overline{\tilde{a}(0, \nu)} \right\rangle = s\delta_{\mu-\nu}, \qquad \left\langle \tilde{a}(0, \mu)\tilde{a}(0, \nu) \right\rangle = 0, \tag{7}$$

for some positive constant s. It can be shown that the first-order MI approximation is given by (see [33])

$$\left\langle |\tilde{a}(\zeta,\Omega)|^2 \right\rangle \approx s \cdot \frac{M^2(\Omega)+G_1^2(\Omega)+\tilde{\gamma}^2(\Omega)}{4G_1^2(\Omega)} \cdot e^{2G_1(\Omega)\zeta}, \tag{8}$$

where

$$M(\Omega) = \tilde{\beta}_e(\Omega) + 2\tilde{\gamma}_e(\Omega) - 1, \tag{9}$$

$$\Gamma_1(\Omega) = \sqrt{\tilde{\gamma}(\Omega)\tilde{\gamma}(-\Omega) - M^2(\Omega)}, \tag{10}$$

$$G_1(\Omega) = \begin{cases} \Gamma_1(\Omega) & \text{if } \Gamma_1(\Omega) \in \mathbb{R}, \\ 0 & \text{otherwise}, \end{cases} \tag{11}$$

and $\tilde{\beta}_e$ and $\tilde{\gamma}_e$ contain even terms of $\tilde{\beta}$ and $\tilde{\gamma}$, respectively.

Eq. (8) describes how white noise with mean spectral density s is amplified by an MI gain $G_1(\Omega)$. Modulation instability analysis, however, suffers from several shortcomings. Since higher-order nonlinear interactions are neglected, expressions so far cannot capture the cascading effect of four-wave mixing.

2.2. *Perturbation* ansatz

Eq. (8) motivates a perturbative approximation to the solution of the form

$$\tilde{a}(\zeta,\Omega) \approx \sum_{n=1}^{\infty} s^{\frac{n}{2}} \Delta_n(\Omega) e^{i\phi_n(\zeta,\Omega)} e^{G_n(\Omega)\zeta}, \tag{12}$$

where the following random-phase assumption is satisfied

$$\left\langle e^{i\phi_n(x,\mu)} e^{-i\phi_m(y,\nu)} \right\rangle = \delta_{n,m}\delta(x-y)\delta(\mu-\nu), \tag{13}$$

Note that, to a first order, Eq. (12) agrees with Eq. (8) with G_1 given by Eq. (11) and, for $G_1(\Omega) \neq 0$,

$$\left\langle |\Delta_1(\Omega)|^2 \right\rangle = \frac{M^2(\Omega)+G_1^2(\Omega)+\tilde{\gamma}^2(\Omega)}{4G_1^2(\Omega)}. \tag{14}$$

If we also assume that Δ_n are independent of ϕ_m for all n, m, Δ_n is independent of Δ_m for $m \neq n$, and G_n is deterministic and real, the mean squared value of the perturbation must evolve as

$$\left\langle |\tilde{a}(\zeta,\Omega)|^2 \right\rangle \approx \sum_{n=1}^{\infty} s^n \left\langle |\Delta_n(\Omega)|^2 \right\rangle e^{2G_n(\Omega)\zeta}. \tag{15}$$

In order to find expressions for $\langle |\Delta_n(\Omega)|^2 \rangle$ and $G_n(\Omega)$, we substitute Eq. (12) in Eqs. (3)–(4) and use Eq. (15). However, to make calculations tractable and final expressions simpler, we propose several simplifying hypotheses which are detailed in Appendix A. Although the true extent of their effect can only be comprehended in the context of the detailed calculations presented in the appendix, some of these simplifications are easy to understand:

1. We assume that the functions $G_n(\Omega)$ are even. This assumption is motivated by the fact that $G_1(\Omega)$ (the MI gain) is even.
2. We also assume that $\langle |\Delta_n(\Omega)|^2 \rangle$ are even functions. Again, this simplification is motivated by the modulation instability case: as it can be shown, from Eq. (14), $\langle |\Delta_1(\Omega)|^2 \rangle$ is even.
3. We neglect the interaction of higher-order MI terms: we only keep the interaction of $n \rangle 1$ terms in Eq. (12) with the modulation instability ($n = 1$) term.
4. We also neglect three-fold interactions of terms in Eq. (12).
5. Substitution of Eq. (12) in Eq. (6) leads to a number of convolution integrals. We consider that the weight of the corresponding integrands is maximized when the exponents $(G_1(u) + G_{n-1}(u-\nu))$ and $G_1(u) + G_{n-1}(\nu - u))$ are maximized. This approximation is very important to obtain simple expressions for G_n, as it is explained in Appendix A.
6. Finally, we repeatedly use Eq. (13), we use the fact that $\left\langle \partial_\zeta \phi_n(\zeta,\Omega) \right\rangle = 0$ and neglect higher-order moments of $\partial_\zeta \phi_n(\zeta, \pm\Omega)$.

After some lengthy manipulations, we arrive at the following expressions:

$$G_n(\Omega) = \max_u G_1(u) + G_{n-1}(u - \Omega), \tag{16}$$

$$\left\langle |\Delta_n(\Omega)|^2 \right\rangle = \frac{\alpha^{n-1}\tilde{\gamma}^2(\Omega) \cdot \left[|B(-\Omega) - iG_n(\Omega)|^2 + \tilde{\gamma}^2(-\Omega) \right]}{|(B(\Omega)+iG_n(\Omega))(B(\Omega)-iG_n(\Omega)) - \tilde{\gamma}(\Omega)\tilde{\gamma}(-\Omega)|^2}. \tag{17}$$

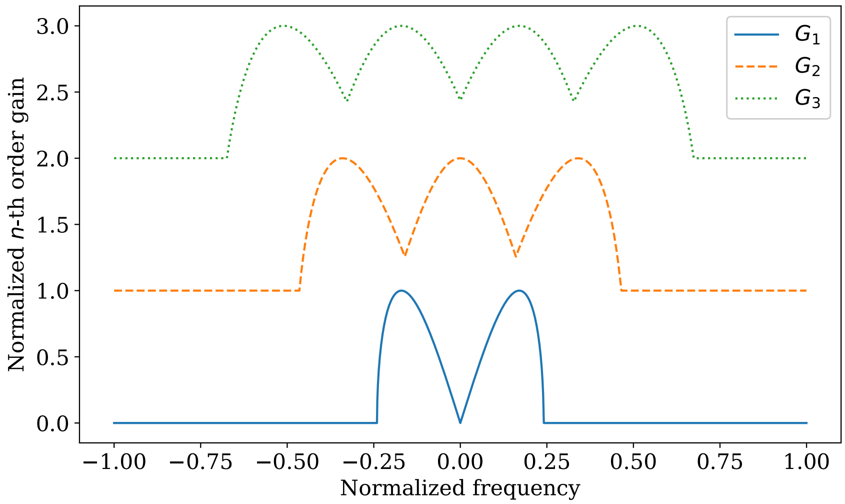

Fig. 1. G_1, G_2 and G_3. The cascading four-wave mixing process is readily observed.

The positive constant α in Eq. (17) is related to the MI gain bandwidth.

Although Eq. (15) correctly describes the evolution of the perturbation, it is not accurate at $\zeta = 0$. Indeed, as it can be readily calculated,

$$\left\langle |\tilde{a}(0,\Omega)|^2 \right\rangle \approx \sum_{n=1}^{\infty} s^n \left\langle |\Delta_n(\Omega)|^2 \right\rangle. \tag{18}$$

This equation does not lead to the known value $\left\langle |\tilde{a}(0,\Omega)|^2 \right\rangle = s$. Eq. (15) can be made accurate even at $\zeta = 0$, that is, for the initial random pertubation, by making a minor correction to Eq. (12):

$$\left\langle |\tilde{a}(\zeta,\Omega)|^2 \right\rangle \approx s + \sum_{n=1}^{\infty} s^n \left\langle |\Delta_n(\Omega)|^2 \right\rangle \left(e^{2G_n(\Omega)\zeta} - 1 \right). \tag{19}$$

2.3. Discussion

Eq. (16) is a result of the cascading effect of four-wave mixing. Fig. 1 shows an example of G_i for $i = 1, 2, 3$ that helps understand the cascading effect when perturbations attain enough power and themselves act as new pumps. The resulting higher-order MI sidebands have already been discussed in the literature. Erkintalo et al. [22], for example, describe how an Akhmediev-breather evolves and splits into subpulses using the Darboux transformation and demonstrate a good agreement with experimental results. While Ref. [22] develops higher-order solutions by iteratively applying the Darboux transformation, Zakharov et al. [29] present a class of multisolitonic solutions which may be used to describe MI development. Kimmoun et al. [39] study a similar higher-order cascading process in surface gravity waves in deep-water and Armaroli et al. [40] also analyze the second-order sidebands in the case of the Dysthe equation.

For the sake of simplicity, we have omitted the influence of stimulated Raman scattering. However, simple modifications to the formulas presented here allow to incorporate in straightforward fashion the molecular Raman response of the medium.

It must be noted that the proposed approximation assumes that the CW pump acts as an unlimited source of optical power. As a matter of fact, Eq. (19) predicts a continuous growth of the perturbation. Since the power of the perturbation cannot exceed that of the pump at the input end of the optical fiber, the proposed analytical model does not apply to an arbitrary long propagated distance ζ, a shortcoming also present in the linear modulation instability analysis. However, first-order MI analysis does not account for higher-order nonlinear interactions, such as the cascading four-wave mixing and, thus, it fails to give an accurate description of the evolution of the perturbation for even shorter propagation lengths. We verify this assertion in the next Section.

3. Experimental and numerical results

In order to test our approach we performed measurements on a 770 m-long, dispersion-stabilized Highly-Nonlinear Fiber (HNLF) [41]. A CW 30-dBm pump laser at 1590.4 nm was launched at the input end of the fiber. Fig. 2 presents a comparison between the observed power spectral density (measured with 0.1-nm resolution) and the proposed analytical approximation. The latter was obtained by using Eqs. (16), (17) and (19) (adding up to $n = 4$) with $\gamma_0 = 8.7\ \mathrm{W^{-1}Km^{-1}}$, $\gamma_k = 0$ for

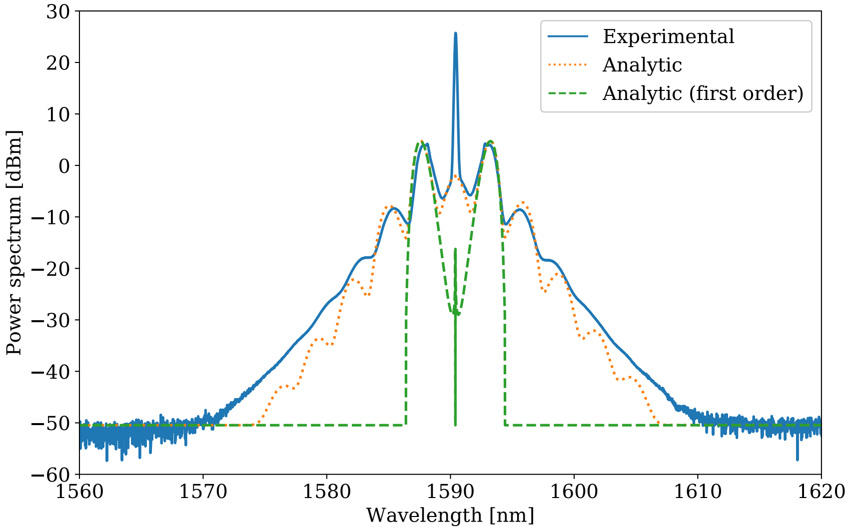

Fig. 2. First-order (dashed line) and fourth-order (dotted line) analytical approximations vs. experimental results (solid line). A CW 30-dBm pump laser at 1590.4 nm was launched at the input end of the 770-m long dispersion-stabilized HNLF.

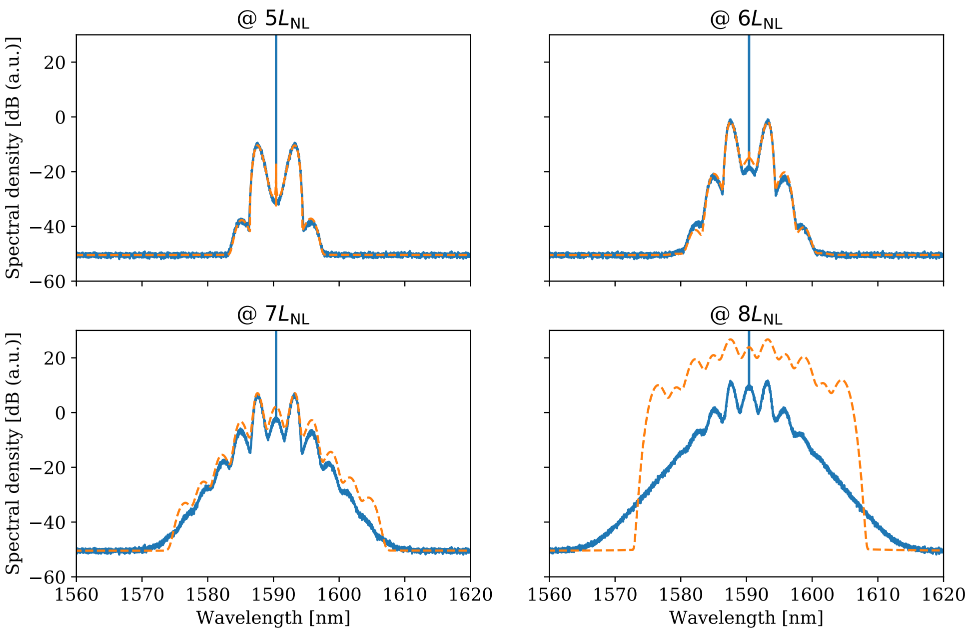

Fig. 3. Analytical approximations (dashed lines) vs. simulation results (solid lines). Numerical results correspond to the average of 100 noise realizations. Results correspond to distances $5L_{\mathrm{NL}}$, $6L_{\mathrm{NL}}$, $7L_{\mathrm{NL}}$, $8L_{\mathrm{NL}}$.

$k\rangle 0$, $\beta_2 = -3.9198$ ps^2/km, $\beta_3 = -0.1267$ ps^3/km, $\beta_4 = 1.7594 \times 10^{-4}$ ps^4/km and $\beta_k = 0$ for $k\rangle 4$. As it is readily observed, experimental and analytical results are in excellent agreement. Fig. 2 also shows the first-order perturbative solution, that is, the solution predicted by the classical modulation instability analysis. MI cannot account for much of the detail observed as it only predicts two gain sidebands.

In order to further explore the validity of the approximations, we performed computer simulations using the algorithm in [42]. Fig. 3 shows results for the average of 100 realizations. The distance is normalized to the so-called nonlinear length $L_{\mathrm{NL}} = (\gamma_0 P_0)^{-1}$, where P_0 is the input power, giving a parameter-independent distance metric. It is observed that the accuracy of the approximation decreases with the propagation distance, although reasonable good results are obtained even after $7L_{\mathrm{NL}}$ ($\approx$800 m).

As it can be seen in the bottom-right panel of Fig. 3, analytical expressions fail to adequately represent the simulated behavior at $8L_{\mathrm{NL}}$. In particular, a limitation of the analytical model becomes apparent; namely, the analytical spectral density has a higher power than that from simulations. As discussed, the analytical model assumes an unlimited pump power source

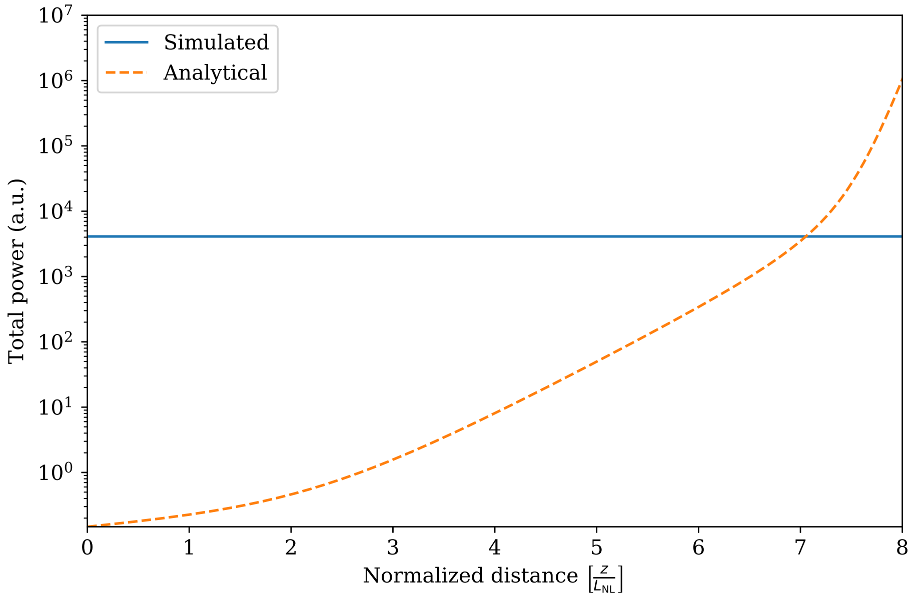

Fig. 4. Total signal power for the analytical approximation (dashed line) vs. simulation (solid line). The crossing at nearly 7 L_{NL} (cf. Fig. 3) marks the maximum propagated distance at which the analytical approximation remains valid.

that enables continuous growth of the perturbation, as shown in Fig. 4 and in accordance with Eq. (19). However, since total power (pump plus perturbation) must remain constant, we can expect the analytical model to be valid as long as the calculated power of the perturbation remains lower than that of the input pump. As shown in Fig. 4, this condition is satisfied up to $\sim 7L_{NL}$, entirely consistent with results in Fig. 3.

4. Conclusions

Modulation instability in nonlinear wave propagation is either approached by means of a linear perturbation analysis to a continuous-wave pump, or by the numerical solution of the Nonlinear Schrödinger equation. While the former approach gives some insight into the initial stages of propagation, it fails at providing an accurate picture over long propagated distances; the latter can provide accurate results over longer distances, but hides the underlying physics.

In this work, we put forth a perturbation analysis that goes beyond the linear modulation instability, offering both a more precise analytical description and meaningful physical insights that capture higher-order cascading four-wave mixing effects. We showed this analysis to be accurate by comparing its predictions to actual experimental results. Furthermore, we successfully validated the approximations made with numerical simulations for propagated distances up to nearly $7L_{NL}$.

The mathematical derivation presented is complex and involves a number of simplifying assumptions but leads to simple and tractable formulas. It is a matter of future work to look for a shorter path and less restrictive simplifications.

In this paper, we do not deal with the nonlinear stage of modulation instability, that is, when the energy of the MI sidebands is comparable to that of the pump. There is also the question of the effect of the particular statistics of the initial perturbation on this stage. These problems are a subject of future research. We study the case of an homogeneous, undoped, single-core and single-mode optical fiber. A more complex setting can be found in, e.g., dual-core [43] and resonant [44] optical fibers.

Finally, we believe our results to be of value when tackling the study of the early stages of supercontinuum generation, and to contribute tools for the better understanding of nonlinear processes such as rogue-wave formation.

Acknowledgments

We gratefully acknowledge S. Radic for hosting J. B.'s research stay at the Photonic Systems Group, UCSD, and E. Temprana for assistance with experiments. We also acknowledge financial support from project PIP 2015, CONICET grant 1122015, 0100001 CO, Argentina.

Appendix A. Mathematical derivation

In order to find expressions for $\langle |\Delta_n(\Omega)|^2 \rangle$ and $G_n(\Omega)$, we substitute Eq. (12) in Eqs. (3)–(4) and use Eq. (15). However, to make the calculations tractable and the final expressions simpler, we resort to several simplifications which were summarized in Section 2.2.

Assuming that the series can be derived term by term, substitution of Eq. (12) into Eqs. (3)–(4)

$$\sum_{n=1}^{\infty} s^{\frac{n}{2}} e^{G_n(\Omega)\zeta} \cdot \mathbf{B} \cdot \begin{bmatrix} \Delta_n(\Omega) e^{i\phi_n(\zeta,\Omega)} \\ \Delta_n^*(-\Omega) e^{-i\phi_n(\zeta,-\Omega)} \end{bmatrix} = -\begin{bmatrix} \tilde{\gamma}(\Omega)\tilde{N}(\tilde{a}(\zeta,\Omega)) \\ \tilde{\gamma}(-\Omega)\overline{\tilde{N}(\tilde{a}(\zeta,-\Omega))} \end{bmatrix}, \tag{A.1}$$

where

$$\mathbf{B} = \begin{bmatrix} B(\Omega) + iG_n(\Omega) - \partial_\zeta \phi_n(\zeta,\Omega) & \tilde{\gamma}(\Omega) \\ \tilde{\gamma}(-\Omega) & B(-\Omega) - iG_n(\Omega) + \partial_\zeta \phi_n(\zeta,-\Omega) \end{bmatrix}. \tag{A.2}$$

In the derivation of Eqs. (A.1)–(A.2) we have made use of the assumption that that the functions $G_n(\Omega)$ are even (simplifying assumption #1 in Section 2.2).

Using Eqs. (6) and (12),

$$\begin{aligned}
\tilde{N}(\tilde{a}(x,\mu)) = \sum_{n=1}^{\infty} s^{\frac{n}{2}} \Bigg\{ & \sum_{m=1}^{n-1} \int_{-\infty}^{+\infty} 2\Delta_m(u)\overline{\Delta_{n-m}(u-\mu)} e^{(G_m(u)+G_{n-m}(u-\mu))x} e^{i(\phi_m(x,u)-\phi_{n-m}(x,u-\mu))} du \\
& + \int_{-\infty}^{+\infty} \Delta_m(u)\Delta_{n-m}(\mu-u) e^{(G_m(u)+G_{n-m}(\mu-u))x} e^{i(\phi_m(x,u)+\phi_{n-m}(x,\mu-u))} du \\
& + \sum_{k=1}^{n-m-1} \int_{-\infty}^{+\infty}\int_{-\infty}^{+\infty} \Delta_m(u)\Delta_k(v)\overline{\Delta_{n-m-k}(u+v-\mu)} \\
& \quad \times e^{(G_m(u)+G_k(u)+G_{n-m-k}(u+v-\mu))x} e^{i(\phi_m(x,u)+\phi_k(x,v)-\phi_{n-m-k}(x,u+v-\mu))} du dv \Bigg\}.
\end{aligned} \tag{A.3}$$

In order to make these equations tractable, we resort to the approximations 3–5 spelled out in Section 2.2. First, approximation #3 implies that we keep only the first term in the sum, that is, $m = 1$. Second, aproximation #4 means that we neglect the terms with double integrals as higher-order perturbations. Finally approximation #5 is, perhaps, the most relevant: we consider that the weight of the integrands is maximized when the exponents $(G_1(u) + G_{n-1}(u-\mu))$ and $(G_1(u) + G_{n-1}(\mu-u))$ are maximized. Since we have already assumed that the G_n are even,

$$\begin{aligned}
\max_u(G_1(u) + G_{n-1}(u-\mu)) &= \max_u(G_1(u) + G_{n-1}(\mu-u)) \\
&= \max_u(G_1(u) + G_{n-1}(\mu+u)) \\
&= \max_u(G_1(u) + G_{n-1}(-\mu-u)).
\end{aligned} \tag{A.4}$$

With all these simplifications, we obtain

$$\tilde{N}(\tilde{a}(x,\mu)) \approx \sum_{n=1}^{\infty} s^{\frac{n}{2}} \cdot e^{\max_u (G_1(u)+G_{n-1}(u-\mu))x} \cdot \{I_1(x,\mu) + I_2(x,\mu)\}, \tag{A.5}$$

where

$$I_1(\zeta,\Omega) = \int_{-\infty}^{+\infty} 2\Delta_1(u)\overline{\Delta_{n-1}(u-\Omega)} e^{i(\phi_1(\zeta,u)-\phi_{n-1}(\zeta,u-\Omega))} du, \tag{A.6}$$

$$I_2(\zeta,\Omega) = \int_{-\infty}^{+\infty} \Delta_1(u)\Delta_{n-1}(\Omega-u) e^{i(\phi_1(\zeta,u)+\phi_{n-1}(\zeta,\Omega-u))} du. \tag{A.7}$$

Using Eqs. (A.4)–(A.7) in Eq. (A.1), we get

$$\sum_{n=1}^{\infty} s^{\frac{n}{2}} \cdot e^{G_n(\Omega)\zeta} \cdot \mathbf{B} \cdot \begin{bmatrix} \Delta_n(\Omega) e^{i\phi_n(\zeta,\Omega)} \\ \Delta_n^*(-\Omega) e^{-i\phi_n(\zeta,-\Omega)} \end{bmatrix} = \sum_{n=1}^{\infty} s^{\frac{n}{2}} \cdot e^{\max_u (G_1(u)+G_{n-1}(u-\Omega))\zeta} \cdot \begin{bmatrix} -\tilde{\gamma}(\Omega)(I_1(\zeta,\Omega) + I_2(\zeta,\Omega)) \\ -\tilde{\gamma}(-\Omega)\left(\overline{I_1}(\zeta,-\Omega) + \overline{I_2}(\zeta,-\Omega)\right) \end{bmatrix}.$$

This equation leads to

$$G_n(\Omega) = \max_u G_1(u) + G_{n-1}(u-\Omega), \tag{A.8}$$

with $G_n(\Omega)$ an even function, and

$$\begin{bmatrix} \Delta_n(\Omega)e^{i\phi_n(\zeta,\Omega)} \\ \Delta_n^*(-\Omega)e^{-i\phi_n(\zeta,-\Omega)} \end{bmatrix} = -\mathbf{B}^{-1}\begin{bmatrix} \tilde{\gamma}(\Omega)(I_1(\zeta,\Omega)+I_2(\zeta,\Omega)) \\ \tilde{\gamma}(-\Omega)\big(\overline{I_1}(\zeta,-\Omega)+\overline{I_2}(\zeta,-\Omega)\big) \end{bmatrix}. \tag{A.9}$$

What remains is to take the mean squared value of $\Delta_n(\Omega)$ which can be found from Eq. (A.9). In the process, a useful simplification is to assume that $\langle|\Delta_n(\Omega)|^2\rangle$ are even functions (as it can be shown, from Eq. (14), that $\langle|\Delta_1(\Omega)|^2\rangle$ is even). We also neglect higher-order moments of $\partial_\zeta\phi_n(\zeta,\pm\Omega)$ and use Eq. (13) (see simplifying assumption #6 in Section 2.2).

From Eq. (A.2),

$$\begin{aligned} -iJ(\Omega)\Delta_n(\Omega)e^{i\phi_n(\zeta,\Omega)} &= \left(-B(-\Omega)+iG_n(\Omega)+\frac{\partial\phi_n(\zeta,\Omega)}{\partial\zeta}\right)\tilde{\gamma}(\Omega)(I_1(\zeta,\Omega)+I_2(\zeta,\Omega)) \\ &\quad -\tilde{\gamma}(\Omega)\tilde{\gamma}(-\Omega)\big(\overline{I_1}(\zeta,-\Omega)+\overline{I_2}(\zeta,-\Omega)\big), \end{aligned} \tag{A.10}$$

where $J(\Omega)=\det(\mathbf{B})$. Multiplying this expression by its conjugate,

$$\begin{aligned} &|J(\Omega)|^2|\Delta_n(\Omega)|^2 = \tilde{\gamma}^2(\Omega)\cdot \\ &\left[\left(-B(-\Omega)+iG_n(\Omega)+\frac{\partial\phi_n(\zeta,-\Omega)}{\partial\zeta}\right)(I_1(\zeta,\Omega)+I_2(\zeta,\Omega))-\tilde{\gamma}(-\Omega)\big(\overline{I_1}(\zeta,-\Omega)+\overline{I_2}(\zeta,-\Omega)\big)\right]\cdot \\ &\left[\left(-B(-\Omega)-iG_n(\Omega)+\frac{\partial\phi_n(\zeta,-\Omega)}{\partial\zeta}\right)\big(\overline{I_1}(\zeta,\Omega)+\overline{I_2}(\zeta,\Omega)\big)-\tilde{\gamma}(-\Omega)(I_1(\zeta,-\Omega)+I_2(\zeta,-\Omega))\right]. \end{aligned} \tag{A.11}$$

Eq. (13) and Eqs. (A.5)–(A.7) lead to

$$\big\langle I_1(\zeta,\Omega)\overline{I_2}(\zeta,\Omega)\big\rangle = \big\langle I_1(\zeta,\Omega)\overline{I_2}(\zeta,-\Omega)\big\rangle = 0, \tag{A.12}$$

$$\big\langle I_1(\zeta,\Omega)\overline{I_1}(\zeta,\Omega)\big\rangle = \big\langle I_2(\zeta,\Omega)\overline{I_2}(\zeta,-\Omega)\big\rangle = 0, \tag{A.13}$$

$$\big\langle|I_1(\zeta,\Omega)|^2\big\rangle = \int_{-\infty}^{+\infty} 4\big\langle|\Delta_1(u)|^2\big\rangle\big\langle|\Delta_{n-1}(u-\Omega)|^2\big\rangle du, \tag{A.14}$$

$$\big\langle|I_1(\zeta,-\Omega)|^2\big\rangle = \int_{-\infty}^{+\infty} 4\big\langle|\Delta_1(u)|^2\big\rangle\big\langle|\Delta_{n-1}(u+\Omega)|^2\big\rangle du, \tag{A.15}$$

$$\big\langle|I_2(\zeta,\Omega)|^2\big\rangle = \int_{-\infty}^{+\infty} \big\langle|\Delta_1(u)|^2\big\rangle\big\langle|\Delta_{n-1}(\Omega-u)|^2\big\rangle du, \tag{A.16}$$

$$\big\langle|I_2(\zeta,-\Omega)|^2\big\rangle = \int_{-\infty}^{+\infty} \big\langle|\Delta_1(u)|^2\big\rangle\big\langle|\Delta_{n-1}(-\Omega-u)|^2\big\rangle du. \tag{A.17}$$

Using simplification #2 in Section 2.2 (i.e, assume that $\langle|\Delta_n(\Omega)|^2\rangle$ are even functions), we may write

$$\big\langle|I_1(\zeta,\Omega)|^2\big\rangle+\big\langle|I_2(\zeta,\Omega)|^2\big\rangle = \big\langle|I_1(\zeta,-\Omega)|^2\big\rangle+\big\langle|I_2(\zeta,-\Omega)|^2\big\rangle = 5\int_{-\infty}^{+\infty}\big\langle|\Delta_1(u)|^2\big\rangle\big\langle|\Delta_{n-1}(u-\Omega)|^2\big\rangle du. \tag{A.18}$$

Finally, using approximation #6 in Section 2.2,

$$\big\langle|J(\Omega)|^2|\Delta_n(\Omega)|^2\big\rangle = \tilde{\gamma}^2(\Omega)\cdot\big[|B(-\Omega)-iG_n(\Omega)|^2+\tilde{\gamma}^2(-\Omega)\big]\cdot 5\int_{-\infty}^{+\infty}\big\langle|\Delta_1(u)|^2\big\rangle\big\langle|\Delta_{n-1}(u-\Omega)|^2\big\rangle du. \tag{A.19}$$

Although we may incur in an error, we approximate $\langle|J(\Omega)|^2|\Delta_n(\Omega)|^2\rangle \approx \langle|J(\Omega)|^2\rangle\langle|\Delta_n(\Omega)|^2\rangle$. Using the fact that $\big\langle\partial_\zeta\phi_n(\zeta,\Omega)\big\rangle = 0$ and neglecting higher-order moments of $\partial_\zeta\phi_n(\zeta,\pm\Omega)$ (i.e., simplifying assumption #6 in Section 2.2), we obtain

$$\big\langle|J(\Omega)|^2\big\rangle = |(B(\Omega)+iG_n(\Omega))(B(\Omega)-iG_n(\Omega))-\tilde{\gamma}(\Omega)\tilde{\gamma}(-\Omega)|^2. \tag{A.20}$$

Introducing Eq. (A.20) in Eq. (A.19),

$$\big\langle|\Delta_n(\Omega)|^2\big\rangle \approx \frac{\tilde{\gamma}^2(\Omega)\cdot\big[|B(-\Omega)-iG_n(\Omega)|^2+\tilde{\gamma}^2(-\Omega)\big]}{|(B(\Omega)+iG_n(\Omega))(B(\Omega)-iG_n(\Omega))-\tilde{\gamma}(\Omega)\tilde{\gamma}(-\Omega)|^2}\cdot 5\int_{-\infty}^{+\infty}\big\langle|\Delta_1(u)|^2\big\rangle\big\langle|\Delta_{n-1}(u-\Omega)|^2\big\rangle du. \tag{A.21}$$

By the way we defined Δ_1 (see Eq. (14)), the integral is actually a definite integral. Since the integrands are nonnegative, by the mean-value theorem we may write

$$\int_{-\infty}^{+\infty} \left\langle |\Delta_1(u)|^2 \right\rangle \left\langle |\Delta_{n-1}(u-\Omega)|^2 \right\rangle du = \left\langle |\Delta_{n-1}(c(\Omega))|^2 \right\rangle \int_{-\infty}^{+\infty} \left\langle |\Delta_1(u)|^2 \right\rangle du. \tag{A.22}$$

This equation motivates our last simplification. Let us define

$$\Lambda_n = 5 \int_{-\infty}^{+\infty} \left\langle |\Delta_1(u)|^2 \right\rangle \left\langle |\Delta_{n-1}(u-\Omega)|^2 \right\rangle du. \tag{A.23}$$

We assume that

$$\Lambda_n \approx \alpha \Lambda_{n-1} \text{ for } n > 1, \qquad \Lambda_1 = 1. \tag{A.24}$$

Using this approximation, we have

$$\left\langle |\Delta_n(\Omega)|^2 \right\rangle \approx \alpha^{n-1} \cdot \frac{\tilde{\gamma}^2(\Omega) \cdot \left[|B(-\Omega) - iG_n(\Omega)|^2 + \tilde{\gamma}^2(-\Omega) \right]}{\left| (B(\Omega) + iG_n(\Omega))(B(\Omega) - iG_n(\Omega)) - \tilde{\gamma}(\Omega)\tilde{\gamma}(-\Omega) \right|^2}. \tag{A.25}$$

In practice, α may help compensate some of the approximations in the derivation of Eq. (A.25) and needs to be estimated for each particular scenario.

References

[1] Agrawal G. Nonlinear fiber optics. Optics and Photonics. 5th ed. Academic Press; 2012.
[2] Zakharov VE. Collapse of langmuir waves. Soviet Phys JETP 1972;35:908–14.
[3] Ablowitz MA, Clarkson PA. Solitons, nonlinear evolution equations and inverse scattering. Cambridge University Press; 1991. ISBN 978-0521387309.
[4] Akhmediev N, Korneev V. Modulation instability and periodic solutions of the nonlinear Schrödinger equation. Theor Math Phys 1986;69(2):1089–93.
[5] Dudley JM, Genty G, Dias F, Kibler B, Akhmediev N. Modulation instability, Akhmediev breathers and continuous wave supercontinuum generation. Opt Express 2009;17(24):21497–508. doi:10.1364/OE.17.021497.
[6] Akhmediev N, Soto-Crespo JM, Ankiewicz A. How to excite a rogue wave. Phys Rev A 2009;80:043818. doi:10.1103/PhysRevA.80.043818.
[7] Akhmediev N, Ankiewicz A, Taki M. Waves that appear from nowhere and disappear without a trace. Phys Lett A 2009;373(6):675–8. doi:10.1016/j.physleta.2008.12.036.
[8] Ankiewicz A, Soto-Crespo JM, Chowdhury MA, Akhmediev N. Rogue waves in optical fibers in presence of third-order dispersion, self-steepening, and self-frequency shift. J Opt Soc Am B 2013;30(1):87–94. doi:10.1364/JOSAB.30.000087.
[9] Ankiewicz A, Akhmediev N. Higher-order integrable evolution equation and its soliton solutions. Phys Lett A 2014;378(4):358–61. doi:10.1016/j.physleta.2013.11.031.
[10] Ankiewicz A, Wang Y, Wabnitz S, Akhmediev N. Extended nonlinear Schrödinger equation with higher-order odd and even terms and its rogue wave solutions. Phys Rev E 2014;89:012907. doi:10.1103/PhysRevE.89.012907.
[11] Ankiewicz A, Kedziora DJ, Chowdury A, Bandelow U, Akhmediev N. Infinite hierarchy of nonlinear Schrödinger equations and their solutions. Phys Rev E 2016;93:012206. doi:10.1103/PhysRevE.93.012206.
[12] Hult J. A fourth-order runge-kutta in the interaction picture method for simulating supercontinuum generation in optical fibers. J Lightwave Technol 2007;25(12):3770–5. doi:10.1109/JLT.2007.909373.
[13] Benjamin TB, Feir JE. The disintegration of wave trains on deep water part 1. theory. J Fluid Mech 1967;27:417–30. doi:10.1017/S002211206700045X.
[14] Hasegawa A. Observation of self-trapping instability of a plasma cyclotron wave in a computer experiment. Phys Rev Lett 1970;24:1165–8. doi:10.1103/PhysRevLett.24.1165.
[15] Zakharov V, Shabat A. Exact theory of two-dimensional self-focusing and one-dimensional self-modulation of waves in nonlinear media. Soviet Phys JETP 1972;34:62–9.
[16] Hasegawa A, Brinkman W. Tunable coherent IR and FIR sources utilizing modulational instability. IEEE J Quantum Electron 1980;16(7):694–7. doi:10.1109/JQE.1980.1070554.
[17] Janssen PAEM. Modulational instability and the fermi-pasta-ulam recurrence. Phys Fluids 1981;24(1):23–6. doi:10.1063/1.863242.
[18] Anderson D, Lisak M. Modulational instability of coherent optical-fiber transmission signals. Opt Lett 1984;9(10):468–70. doi:10.1364/OL.9.000468.
[19] Shukla PK, Rasmussen JJ. Modulational instability of short pulses in long optical fibers. Opt Lett 1986;11(3):171–3. doi:10.1364/OL.11.000171.
[20] Tai K, Hasegawa A, Tomita A. Observation of modulational instability in optical fibers. Phys Rev Lett 1986;56:135–8. doi:10.1103/PhysRevLett.56.135.
[21] Potasek MJ. Modulation instability in an extended nonlinear Schrödinger equation. Opt Lett 1987;12(11):921–3. doi:10.1364/OL.12.000921.
[22] Erkintalo M, Hammani K, Kibler B, Finot C, Akhmediev N, Dudley JM, et al. Higher-order modulation instability in nonlinear fiber optics. Phys Rev Lett 2011;107:253901. doi:10.1103/PhysRevLett.107.253901.
[23] Solli D, Herink G, Jalali B, Ropers C. Fluctuations and correlations in modulation instability. Nat Photonics 2012;6(7):463–8.
[24] Grosz D, Mazzali C, Celaschi S, Paradisi A, Fragnito H. Modulation instability induced resonant four-wave mixing in WDM systems. IEEE Photonics Technol Lett 1999;11(3):379–81. doi:10.1109/68.748242.
[25] Grosz D, Boggio JC, Fragnito H. Modulation instability effects on three-channel optically multiplexed communication systems. Opt Commun 1999;171(1–3):53–60. doi:10.1016/S0030-4018(99)00494-0.
[26] Hammani K, Wetzel B, Kibler B, Fatome J, Finot C, Millot G, et al. Spectral dynamics of modulation instability described using Akhmediev breather theory. Opt Lett 2011;36(11):2140–2. doi:10.1364/OL.36.002140.
[27] Sørensen ST, Larsen C, Møller U, Moselund PM, Thomsen CL, Bang O. Influence of pump power and modulation instability gain spectrum on seeded supercontinuum and rogue wave generation. J Opt Soc Am B 2012;29(10):2875–85. doi:10.1364/JOSAB.29.002875.
[28] Soto-Crespo JM, Ankiewicz A, Devine N, Akhmediev N. Modulation instability, cherenkov radiation, and fermi-pasta-ulam recurrence. J Opt Soc Am B 2012;29(8):1930–6. doi:10.1364/JOSAB.29.001930.
[29] Zakharov VE, Gelash AA. Nonlinear stage of modulation instability. Phys Rev Lett 2013;111:054101. doi:10.1103/PhysRevLett.111.054101.
[30] Béjot P, Kibler B, Hertz E, Lavorel B, Faucher O. General approach to spatiotemporal modulational instability processes. Phys Rev A 2011;83:013830. doi:10.1103/PhysRevA.83.013830.
[31] Hernandez SM, Fierens PI, Bonetti J, Sánchez AD, Grosz DF. A geometrical view of scalar modulation instability in optical fibers. IEEE Photonics J 2017;9(5):1–8. doi:10.1109/JPHOT.2017.2754984.
[32] Fierens P, Hernandez S, Bonetti J, Grosz D. On the spectral dynamics of noise-seeded modulation instability in optical fibers. In: In V, Longhini P, Palacios A, editors. Proceedings of the 4th international conference on applications in nonlinear dynamics (ICAND 2016). Springer; 2016. p. 265–76. ISBN 978-3-319-52620-1. doi:10.1007/978-3-319-52621-8_23.

[33] Bonetti J, Hernandez SM, Fierens PI, Grosz DF. Analytical study of coherence in seeded modulation instability. Phys Rev A 2016;94:033826. doi:10.1103/PhysRevA.94.033826.
[34] Zakharov V, Dias F, Pushkarev A. One-dimensional wave turbulence. Phys Rep 2004;398(1):1–65. doi:10.1016/j.physrep.2004.04.002.
[35] Picozzi A, Pitois S, Millot G. Spectral incoherent solitons: a localized soliton behavior in the frequency domain. Phys Rev Lett 2008;101:093901. doi:10.1103/PhysRevLett.101.093901.
[36] Picozzi A, Rica S. Condensation of classical optical waves beyond the cubic nonlinear Schrödinger equation. Opt Commun 2012;285(24):5440–8.
[37] Picozzi A, Garnier J, Hansson T, Suret P, Randoux S, Millot G, et al. Optical wave turbulence: towards a unified nonequilibrium thermodynamic formulation of statistical nonlinear optics. Phys Rep 2014;542(1):1–132. doi:10.1016/j.physrep.2014.03.002.
[38] Soto-Crespo JM, Devine N, Akhmediev N. Integrable turbulence and rogue waves: breathers or solitons? Phys Rev Lett 2016;116:103901. doi:10.1103/PhysRevLett.116.103901.
[39] Kimmoun O, Hsu HC, Kibler B, Chabchoub A. Nonconservative higher-order hydrodynamic modulation instability. Phys Rev E 2017;96(2):022219. doi:10.1103/physreve.96.022219.
[40] Armaroli A, Brunetti M, Kasparian J. Recurrence in the high-order nonlinear Schrödinger equation: a low-dimensional analysis. Phys Rev E 2017;96:012222. doi:10.1103/PhysRevE.96.012222.
[41] Kuo BP-P, Fini JM, Grüner-Nielsen L, Radic S. Dispersion-stabilized highly-nonlinear fiber for wideband parametric mixer synthesis. Opt Express 2012;20(17):18611–19. doi:10.1364/OE.20.018611.
[42] Travers JC, Frosz MH, Dudley JM. Nonlinear fibre optics overview. In: Dudley JM, Taylor JR, editors. Supercontinuum generation in optical fibers. Cambridge University Press; 2010. p. 32–51.
[43] Ganapathy R, Malomed BA, Porsezian K. Modulational instability and generation of pulse trains in asymmetric dual-core nonlinear optical fibers. Phys Lett A 2006;354(5–6):366–72. doi:10.1016/j.physleta.2006.02.002.
[44] Kalithasan B, Porsezian K, Dinda PT, Malomed BA. Modulational instability and generation of self-induced transparency solitons in resonant optical fibers. J Opt A 2009;11(4):045205. doi:10.1088/1464-4258/11/4/045205.